



This is a repository copy of *Double-layer-gate architecture for few-hole GaAs quantum dots*.

White Rose Research Online URL for this paper:  
<http://eprints.whiterose.ac.uk/103204/>

Version: Accepted Version

---

**Article:**

Wang, D.Q., Hamilton, A.R., Farrer, I. [orcid.org/0000-0002-3033-4306](https://orcid.org/0000-0002-3033-4306) et al. (2 more authors) (2016) Double-layer-gate architecture for few-hole GaAs quantum dots. *Nanotechnology*, 27 (33). ISSN 0957-4484

<https://doi.org/10.1088/0957-4484/27/33/334001>

---

This is an author-created, un-copyedited version of an article accepted for publication/published in *Nanotechnology*. IOP Publishing Ltd is not responsible for any errors or omissions in this version of the manuscript or any version derived from it. The Version of Record is available online at <http://dx.doi.org/10.1088/0957-4484/27/33/334001>.

**Reuse**

Unless indicated otherwise, fulltext items are protected by copyright with all rights reserved. The copyright exception in section 29 of the Copyright, Designs and Patents Act 1988 allows the making of a single copy solely for the purpose of non-commercial research or private study within the limits of fair dealing. The publisher or other rights-holder may allow further reproduction and re-use of this version - refer to the White Rose Research Online record for this item. Where records identify the publisher as the copyright holder, users can verify any specific terms of use on the publisher's website.

**Takedown**

If you consider content in White Rose Research Online to be in breach of UK law, please notify us by emailing [eprints@whiterose.ac.uk](mailto:eprints@whiterose.ac.uk) including the URL of the record and the reason for the withdrawal request.



[eprints@whiterose.ac.uk](mailto:eprints@whiterose.ac.uk)  
<https://eprints.whiterose.ac.uk/>

# Double-layer-gate architecture for few-hole GaAs quantum dots

**D. Q. Wang**

School of Physics, University of New South Wales, Sydney NSW 2052, Australia

**I. Farrer<sup>†</sup>**

Cavendish Laboratory, J. J. Thomson Avenue, Cambridge, CB3 0HE, United Kingdom

**D. A. Ritchie**

Cavendish Laboratory, J. J. Thomson Avenue, Cambridge, CB3 0HE, United Kingdom

**A. R. Hamilton**

School of Physics, University of New South Wales, Sydney NSW 2052, Australia

**O. Klochan**

School of Physics, University of New South Wales, Sydney NSW 2052, Australia

E-mail: [O.Klochan@unsw.edu.au](mailto:O.Klochan@unsw.edu.au)

**Abstract.** We report the fabrication of single and double hole quantum dots using a double-layer-gate design on an undoped accumulation mode  $\text{Al}_x\text{Ga}_{1-x}\text{As}/\text{GaAs}$  heterostructure. Electrical transport measurements of a single quantum dot show varying addition energies and clear excited states. In addition, the two-level-gate architecture can also be configured into a double quantum dot with tunable inter-dot coupling.

<sup>†</sup> Present Address: School of Electrical Engineering, University of Sheffield, Western Bank, Sheffield, S10 2TN, United Kingdom

Long-lived heavy-hole spins have drawn significant attention recently due to the suppressed hyperfine interaction with surrounding nuclei [1, 2, 3, 4, 5, 6], which is the main mechanism leading to fast decoherence ( $\sim 10$  ns) of electron spins [7, 8]. Recent theoretical studies suggest the dephasing time  $T_2^*$  for holes to be in the range of  $\mu s$ , with an Ising-like hyperfine interaction [3, 4]. Optical measurements of self-assembled quantum dots have shown varied results, with  $T_2^* > 100$  ns from coherent population measurements [9], and  $T_2^*$  up to 20 ns from Ramsey fringes [10, 11]. The short  $T_2^*$  was shown not to be limited by nuclear spins, but by charge noise [11].

The promising optical measurements described above indicate that hole spins in gate defined quantum dots should be investigated. However, due to the large effective mass ( $m_h^*/m_e^* \sim 3 - 13$ ) [12], hole quantum dots need to have much smaller dimensions compared to electron dots to show similar single particle energy scales since the orbital energies  $E_{orb} \sim 1/m^*A_{dot}$ , which is hard to achieve by simply duplicating the design for electron quantum dots. Even though the operation of GaAs single hole transistors has been demonstrated [13, 14, 15], to date it has not been possible to observe Zeeman splitting of the single particle levels, which is a prerequisite for measurements of the  $T_1$  and  $T_2^*$  spin lifetimes, and for coherent spin manipulation.

In this paper, we present a double-layer-gate design that allows formation of both single and double hole quantum dots. By further shrinking the lithographic dimensions of the dot, we show that a few-hole quantum dot with varying addition energy can be defined. In a perpendicular magnetic field, we also observe Zeeman splitting of the hole states, from which we extract the hole  $g$ -factor.

The hole quantum dot is fabricated on a shallow undoped (100) GaAs/ $Al_xGa_{1-x}As$  heterostructure comprising a 10 nm GaAs cap and a 50 nm  $Al_xGa_{1-x}As$  layer on a GaAs buffer layer using the approach described in Ref [17]. Separate measurements of a 2D Hall bar device show the 2D holes have a mobility of  $600,000$   $cm^2/Vs$  at  $p = 2.5 \times 10^{11}$   $cm^{-2}$  and  $T = 250$  mK. The quantum dot architecture has a double-layer-gate design: firstly, three parallel barrier gates are deposited directly on top of the wafer, then a 30 nm  $AlO_x$  dielectric is deposited using atomic layer deposition, and finally a 150 nm wide top-gate is deposited over the barrier

gates. Figure 1(a) shows an SEM image of the device where the three barrier gates are labelled as 1, 2, 3 respectively and the top-gate channel labelled as TG.

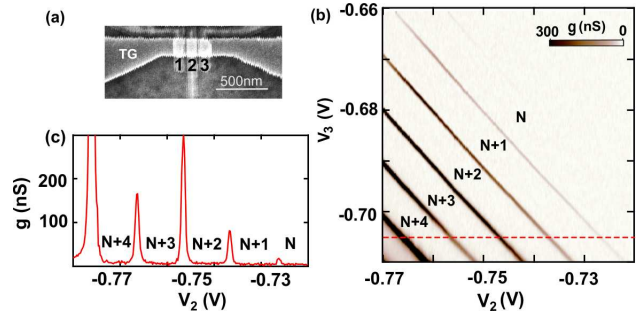


**Figure 1.** (a) A Scanning Electron Microscope (SEM) image of the device showing the double-layer design. Three barrier gates are on the bottom layer (labelled 1, 2, 3) and have a width of 40nm and a inter-gate spacing of 80nm. The top-gate channel (labelled TG) is on the top layer and has a width of 150 nm; (b) Conductance  $g$  of the dot measured as a function of the voltages on gate 2 and 3 when gate 1 is lifted to  $V_1 = -0.9$  V, showing the formation of a single quantum dot in between the two barrier gates 2 and 3. (c) Differential conductance  $g$  of the dot as a function of the gate voltage  $V_2$  along the red dashed line in (b).

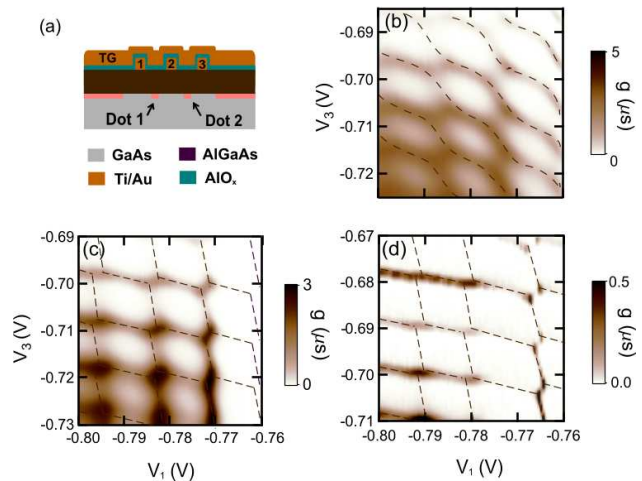
The device was measured in a dilution refrigerator with a base hole temperature of 80 mK using standard lock-in techniques and an AC excitation of  $15$   $\mu V$ . When the top-gate (TG) is negatively biased, holes accumulate at the heterointerface forming a 1D channel. Tuning the voltages on the barrier gates confines the 1D hole channel into isolated islands, i.e. quantum dots. With the flexibility of three parallel barrier gates, the device can be tuned into either a single quantum dot using any two consecutive barriers while lifting the third, or a double quantum dot using all three barriers. We first show data from a single dot configuration with the top-gate used to induce holes into the dot ( $V_{TG} = -3.1$  V) and gate 2 and 3 biased to define barriers of the dot as well as control the dot occupation. Gate 1 is made transparent ( $V_1 = -0.9$  V) and forms part of the lead. Figure 1(b) shows the conductance  $g=dI/dV$  of the dot as a function of the voltages on gate 2 and 3. The lines in Figure 1(b) are almost at  $45^\circ$ , indicating formation of a single quantum dot which has almost the same capacitive coupling to the two gates 2 and 3, and thus must be located half way between the two barriers. Figure 1(c) plots the

conductance of the dot along the red dashed line in Figure 1(b) showing the Coulomb oscillation peaks as the voltage on gate 2 ( $V_2$ ) is varied. As the local dot potential is tuned by the bias  $V_2$ , a conductance peak is measured whenever a hole is added or removed from the dot. The Coulomb blockade peaks are fairly evenly spaced with respect to  $V_2$ , which suggests that the confined dot is in the many-hole limit when the constant charging energy dominates over the varying orbital energy.

An advantage of the double-layer-gate design is the straightforward formation of an additional dot to form a double quantum dot and the simple tuning between single and double dot configurations. With the same device, a double quantum dot can be easily configured by bringing down the voltage on gate 1. Similar to the operation of gate 2 and 3, this will also confine another dot in between gate 1 and 2 as shown in Figure 2(a). The conductance of the double dot as a function of voltages on gate 1 and 3 is shown in Figure 2(b)-(d) as coupling between the two dots is controlled by the voltage  $V_2$  on the middle barrier gate. In Figure 2, we show three regimes of inter-dot coupling: (b) strongly coupled double dot with curving diagonal parallel lines resembling Figure 1(c), indicating the two dots are merging into one; (c) intermediate coupled double dot with standard honeycomb pattern; and (d) weakly coupled double dot with leakage current greatly suppressed and only transport through triple points visible. The ability to configure double hole quantum dots with tunable inter-dot coupling suggests this device design will allow more complicated double dot measurements and spin-dependent transport.

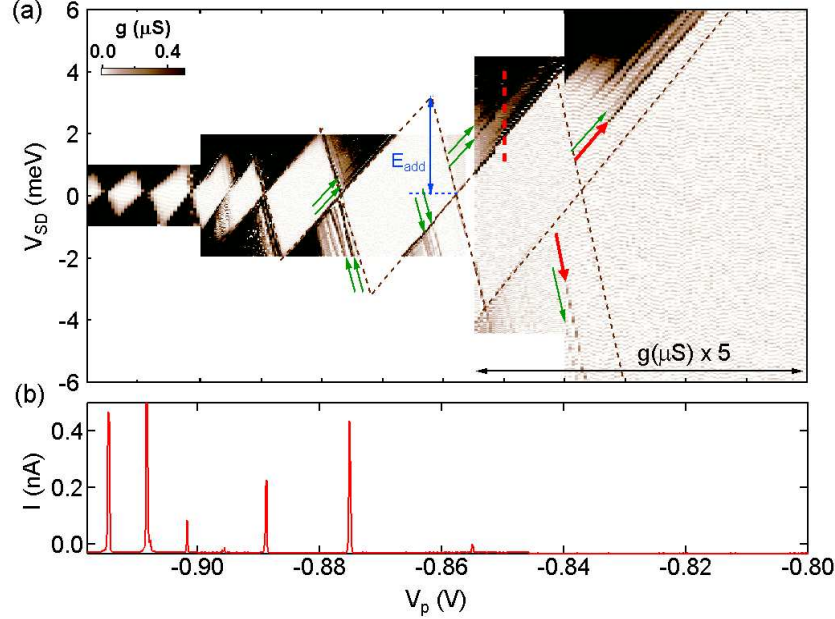
Another advantage of the double-layer-gate design is the flexibility in changing the dot dimensions. The width and spacing of the finger gates, as well as the width of the top-gate channel can both be easily reduced to confined a much smaller dot. Figure 3 shows the bias spectroscopy and Coulomb blockade peaks measured from a smaller dot with reduced dimensions: the finger gates now have a width of 30 nm and a spacing of 50 nm. The width of the top-gate channel is also reduced from 150 nm to 50 nm. In the new small dot, gate 1 and gate 3 are used as the left and right barriers of the dot while gate 2 is used as the plunger gate to vary the number of holes on the dot. 30 nm of  $\text{AlO}_x$  is also used as the dielectric for the ohmic region but etched down to 10 nm in the active dot region to avoid overgrowth of the oxide in between the narrow finger gates when their spacing is reduced.

Figure 3(a) shows the bias spectroscopy diagram of the new dot with reduced dimensions, and Figure 3(b) plots the corresponding Coulomb blockade peaks at zero bias. In Figure 3(a), the differential



**Figure 2.** (a) A side-view schematic of the device showing the double dot configuration. (b) Conductance  $g$  as a function of voltages on barrier gate 1 and 3 for strongly coupled double dot ( $V_2 = -0.80$  V); (c) for intermediately coupled double dot ( $V_2 = -0.79$  V); (c) and for weakly coupled double dot ( $V_2 = -0.78$  V).

conductance through the dot is plotted as a function of the source-drain bias and the plunger gate voltage. From the half size of the Coulomb diamonds as illustrated by the blue arrows in Figure 3(a), the energy  $E_{add}$  required to add each hole to the dot can be extracted. The addition energy of the dot  $E_{add}$  fluctuates while gradually increases from 1 meV to 4 meV, which suggests the dot is operating in the few-hole regime [25]. Figure 3(b) plots the corresponding Coulomb blockade peaks at zero bias, the varying periodicity of which also reflects the fluctuating energy required to add or remove each hole from the dot. As well as the varying Coulomb blockade period, information about the orbital energy of the dot can also be extracted from the bias spectroscopy diagram. The differential conductance peaks running parallel to the edges of the Coulomb diamonds, highlighted by the arrows in Figure 3(a), originate from transport through the excited orbital states within the dot. Those conductance peaks appear at the same energy in both positive and negative source-drain bias directions, which excludes the possibility that they are caused by resonance of the dot state with the 1D states in the lead. Other closely spaced fine conductance peaks parallel to the edges of the diamonds, which only appear in one bias direction, most likely originate from the states in the 1D lead. Since we are only interested in the energy states of the dot, here we focus on the conductance peaks highlighted by the arrows. From the excited states indicated by the red arrows, we extract the orbital level spacing to be around 1 meV. This orbital energy scale is comparable to that



**Figure 3.** (a) Bias spectroscopy diagram of the single quantum dot with shrunk size: differential conductance  $g=dI/dV_{SD}$  through the dot is plotted as a function of the source-drain bias and the plunger gate voltage  $V_p$ . The differential conductance  $g$  is magnified for  $V_p > -0.855$  V to show the last visible diamond. Green and red arrows highlight the conductance peaks correspond to transport through excited states. (b) The corresponding Coulomb blockade peaks of the dot: current through the dot at zero bias is plotted as a function of the plunger gate voltage  $V_p$ .

of 2D GaAs electron quantum dots with similar charge occupation [16], in which single electron spin properties have been extensively studied. It is also worth pointing out that a large orbital energy is only achievable when the hole dot size is significantly reduced compared to its electron counterpart given the mismatch between the heavy hole and electron effective masses in GaAs ( $m_h^*/m_e^* \sim 3 - 13$ ) [12]. Using  $A_{dot} = 2\pi\hbar^2/E_{orb}m_h^*$  and  $m_h^* = 0.2m_0$ , we estimate the dot diameter to be around 40 nm assuming a circular dot. The electrical size of the dot is significantly smaller than that has been achieved with conventional single layer gate designs [16, 13, 15]. Owing to the reduced dot size, we are able to achieve single hole energy level spacings much larger than  $4k_B T$ , which is necessary to study splitting of hole spin states in lateral quantum dots.

To explore the splitting of the hole states, we introduce a magnetic field  $B$  perpendicular to the heterostructure while monitoring the energy states crossing the red dashed line in Figure 3(a) (i.e. at  $V_p = -0.85$  V). Splitting of the orbital states is observed as depicted in Figure 4(a), which plots the differential conductance through the dot at  $V_p = -0.85$  V as a function of the source-drain bias and the magnetic field strength. The measurement is done by stepping the magnetic field from 0 T to 5 T while sweeping the source-drain bias along the red dashed line in

Figure 3(a). The ground state (at  $V_{SD} \sim 2.1$  mV) splits into two distinct lines as the magnetic field is increased. The excited state (at  $V_{SD} \sim 3.2$  mV), on the other hand, exhibits a complicated splitting pattern. This complex splitting of the excited state could result from two closely spaced excited states, or from a fourfold degenerate orbital state [21].

Concentrating on the splitting of the ground state indicated by red arrows in Figure 4(a), we plot in Figure 4(b) the energy difference splitting as a function of the magnetic field. The splitting is linear up to 3T, after which transport through the dot is suppressed by the strong magnetic field. Since the coupling between orbital momentum and magnetic field is not linear, the observed splitting is most likely due to spin effects. If the splitting is assumed to be purely Zeeman energy, the g-factor of the ground state can be extracted to be around 1.4 from a linear fit as depicted in Figure 4(b). The measured g-factor  $g^* = 1.4$  is much smaller than the theoretical 2D value  $g^* = 7.2$  of heavy holes in GaAs, which may be related to the suppression of  $g^*$  observed in 1D GaAs hole systems [22, 23]. This strong suppression of g-factor is possibly a result of the strong confinement potential of the quantum dot, which can change the degree of heavy hole-light hole (HH-LH) mixing in GaAs hole systems [24] and thus modify the magnitude and anisotropy of the g-factor. It is

worth pointing out that splitting of the ground state of a quantum dot generally indicates an odd number of carriers on the dot [16], which suggests that the dot is not empty inside the last observable diamond in Figure 3(a). Transport through quantum dots is often suppressed by opaque barriers as the barriers are pushed to pinch-off in the few-hole regime. Moreover, due to a heavier effective mass, tunnelling of holes is suppressed compared to electrons. Therefore, the suppression of current when  $V_p > -0.82\text{V}$  is most likely caused by significantly reduced hole tunnelling events.

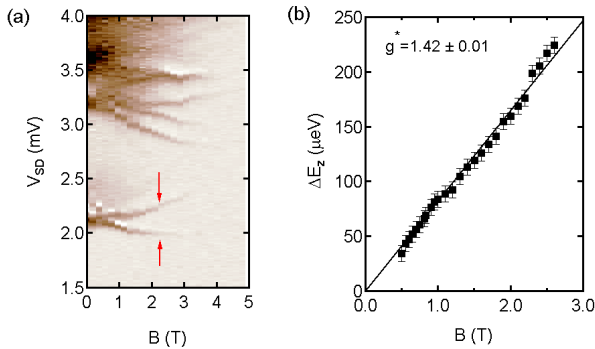


**Figure 4.** (a) Differential conductance through dot measured as a function of the source-drain bias and the perpendicular magnetic field at  $V_p = -0.85\text{V}$ . (b) Energy difference of the split ground states plotted as a function of the magnetic field. An effective g-factor of  $1.42 \pm 0.01$  can be extracted from a linear fit to the energy difference if assuming the splitting is purely Zeeman energy.

In conclusion, we have fabricated both single and double few-hole quantum dots on an undoped  $\text{Al}_x\text{Ga}_{1-x}\text{As}/\text{GaAs}$  heterostructure using a new double-layer-gate design. By shrinking the lithographic dimensions of the dot, we are able to greatly reduce the dot size and the number of holes on the dot to the few-hole regime. Electrical transport measurements through the single quantum dot show clear orbital states with energies comparable to those of lateral electron quantum dots in GaAs. By applying a magnetic field, we also observe splitting of the orbital states, from which an effective g-factor is determined. This device architecture will allow now studies of spin properties and spin lifetimes of holes in quantum dots.

## Acknowledgments

This work is supported by the Australian Research Council (ARC) DP and DECRA Schemes and the EPSRC (UK). All devices were fabricated using facilities at the NSW Node of the Australian National Fabrication Facility (ANFF).

## References

- [1] Chekhovich E A, Makhonin M N, Tartakovskii A I, Yacoby A, Bluhm H, Nowack K C and Vandersypen L M K 2012 *Nature Materials* **12** 494
- [2] Bulaev D V and Loss D 2005 *Phys. Rev. Lett.* **95** 076805
- [3] Fischer J, Coish W A, Bulaev D V and Loss D 2008 *Phys. Rev. B* **78** 155329
- [4] Fischer J and Loss D 2010 *Phys. Rev. Lett.* **105** 266603
- [5] Keane Z K *et al* 2011 *Nano Lett.* **11** 3147
- [6] Klochan O, Hamilton A R, das Gupta K, Sfigakis F, Beere H E and Ritchie D A 2015 *New J. Phys.* **17** 033035
- [7] Petta J R, Johnson A C, Taylor J M, Laird E A, Yacoby A, Lukin M D, Marcus C M, Hanson M P, Gossard A C 2005 *Science* **309** 2180
- [8] Koppens F H L, Buizert C, Tielrooij K J, Vink I T, Nowack K C, Meunier T, Kouwenhoven L P and Vandersypen L M K 2006 *Nature* **442** 766
- [9] Brunner D, Gerardot B D, Galgarno P A, Wüst G, Karrai K, Stoltz N G, Petroff P M, Warburton R J 2009 *Science* **325** 70
- [10] De Greve K, McMahon P L, Press D, Ladd T D, Bisping D, Schneider C, Kamp M, Worschech L, Höfling S, Forchel S and Yamamoto Y 2011 *Nature Phys.* **7** 872
- [11] Greilich A, Carter S G, Kim D, Bracker A S and Gammon D 2011 *Nature Photon.* **5** 702
- [12] Habib B, Shayegan M and Winkler R 2009 *Semicond. Sci. Technol.* **23** 064002
- [13] Komijani Y, Csontos M, Ihn T, Ensslin K, Reuter D and Wieck A D 2008 *EPL* **84** 57004
- [14] Klochan O, Chen J C H, Micolich A P, Hamilton A R, Muraki K and Hirayama Y 2010 *Appl. Phys. Lett.* **96** 092103
- [15] Tracy L A, Hargett T W and Reno J L 2014 *Appl. Phys. Lett.* **104** 123101
- [16] Hanson R, Kouwenhoven L P, Petta J R, Tarucha S and Vandersypen L M K 2007 *Rev. of Mod. Phys.* **79** 1217
- [17] Chen J C H *et al* *Appl. Phys. Lett.* 2012 **100** 052101
- [18] Winkler R 2003 *SpinOrbit Coupling Effects in Two-Dimensional Electron and Hole Systems* (Springer-Verlag Berlin Heidelberg)
- [19] Danneau R *et al* 2006 *Phys. Rev. Lett.* **97** 026403
- [20] Chen J C H, Klochan O, Micolich A P, Hamilton A R, Martin T P, Ho L H, Zülicke U, Reuter D, Wieck A D 2010 *New J. Phys.* **12** 033043
- [21] van der Heijden J, Salfi J, Mol J A, Verduijn J, Tettamanzi G C, Hamilton A R, Collaert N, Rogge S, 2014 *Nano Lett.* **14** 1492
- [22] Srinivasan A, Yeoh L A, Klochan O, Martin T P, Chen J C H, Micolich A P, Hamilton A R, Reuter D and Wieck A D, 2013 *Nano Lett.* **13** 148
- [23] Nichele F, Chesi S, Hennel S, Wittmann A, Gerl C, Wegscheider W, Loss D, Ihn T and Ensslin K 2014 *Phys. Rev. Lett.* **113** 046801
- [24] Csontos D, Brusheim P, Zülicke U and Xu H Q 2009 *Phys. Rev. B* **79** 155323
- [25] Lim W H, Yang C H, Zwanenburg F A and Dzurak A S, 2011 *Nanotechnology* **22** 335704